Ionic Liquid-based Contactors for Carbon Dioxide Removal from Simulated Spacecraft Cabin Atmospheres

James A. Nabity*, Jacob Killelea†, Brett Shaffer‡, Katya Arquilla§, Tessa J. Rundle‡, Trevor J. Fritz‡ and Daniel D. Phillips‡
University of Colorado, Boulder, CO 80303, USA

The ionic liquid, 1-butyl-3-methylimidazolium acetate [bmim][Ac], was used to remove carbon dioxide (CO_2) from a simulated spacecraft cabin atmosphere (2 mm Hg (267 Pa) partial pressure of CO_2 with balance of nitrogen (630 mm Hg total pressure)). Three gas-liquid contactor configurations were experimentally characterized to measure the rates of CO_2 removal from the simulated atmosphere with [bmim][Ac]. Two of the contactors, a parallel path flat plate and hollow fiber membrane, utilized hydrophobic porous membranes (silicone and polypropylene, respectively) to separate the gas and ionic liquid streams. The third, a 3-D printed interior corner capillary-driven contactor was configured for the crossflow of gas directly over the free liquid surface. At circa 90 – 100 mL/min liquid flow and gas flow rate (0.24 slpm), inlet and outlet CO_2 concentration differentials in the gas flow were 990, 2420 and 2680 ± 140 ppm for the flat plate, hollow fiber and interior corner contactors, respectively. For these same contactors, CO_2 removal rates were (18 ± 2) g m^{-2} day^{-1}, (41 ± 3) g m^{-2} day^{-1}, and (60 ± 3) g m^{-2} day^{-1}, respectively. Overall mass transfer coefficients *k* were (5.2 ± 0.3) x 10^{-5} m s-1, (16.8 ± 1.3) x 10^{-5} m s-1 and (25.0 ± 1.9) x 10^{-5} m s-1 for each contactor, respectively. The coefficients generally decreased in direct proportion to increased gas flow. These performance metrics were nearly insensitive to variations in the flow of ionic liquid. The maximum uptake of CO_2 by [bmim][Ac] was measured at 7.45 w% at 630 mm Hg and room temperature (23°C) The loading was 1.67 w% when exposed to the simulated spacecraft cabin atmosphere. In addition, desorption with thermal vacuum and thermal sparge processes were studied at temperatures from 20 to 80°C, the latter using dry inert gases (argon and nitrogen) to remove CO_2 from the ionic liquid. After 4 hrs at 71°C under rough vacuum (0.5 mm Hg) without stirring, gravimetric measurements indicated a decrease in loading of CO_2 from 1.75 w% to 1.29 w%. In comparison, for a 95 mL/min gas sparge flow through CO_2 saturated [bmim][Ac] at 65°C, the loading decreased from 1.67 w% to 0.75 w% over the same period. The results suggest the importance of elevated temperature coupled with agitation to increase the rate of CO_2 desorption from the ionic liquid.

Keywords: carbon dioxide (CO_2) removal, CO_2 sorption / desorption, mass transfer coefficient, 1-butyl-3-methylimidazolium acetate, ionic liquid

Nomenclature

AETHER	Atmospheric and Environmental Test Hub for Experimentation on Revitalization
CaA	Ca^{2+} exchanged zeolite A
c_i	concentration of species i, ppm
D	diffusion coefficient, m^2 s^{-1}
G	mass flux, g m^{-2} day^{-1}
ID	inner diameter, cm
IL	ionic liquid
k	overall mass transfer coefficient, m s-1

* Associate Professor, Department of Smead Aerospace Engineering Sciences, UCB 429. Associate Fellow, AIAA. james.nabity@colorado.edu.
† Undergraduate student, Department of Smead Aerospace Engineering Sciences.
‡ Graduate student, Department of Smead Aerospace Engineering Sciences. Member, AIAA.
§ Graduate student, Department of Smead Aerospace Engineering Sciences.

m	mass, g
MFC	mass flow controller
OD	outer diameter, cm
N	number of acquired samples or readings for a given measurement
$\dot{N}$	molar flux, mol m^{-2} s
p	pressure, Pa
$ppCO_2$	partial pressure of CO_2, Pa
PMP	pump
ppm	parts per million
R_u	universal gas constant, J mol^{-1} K^{-1}
RTIL	room temperature ionic liquid
t	value from Student-t distribution table w/ $\alpha = 0.025$ to attain 95% confidence assuming a two-sided distribution
T	temperature, K
TC	thermocouple
U_Z	the overall uncertainty on calculated parameter Z
x	the measurement of importance (e.g. c_i, m, p, T, etc.)
Z	the derived parameter of interest (e.g. Δc_i, $\dot{N}$, etc.)
δB	bias error
δS	precision error
δx	the measurement uncertainty on x including all sources of error
Δm	change in mass, g
ν	number of degrees of freedom
V	valve
Subscripts	
i	indice for precision errors
j	indice for bias errors

I. Introduction

IN one day, a person exhales about 1 kg of CO_2 [1]. On the International Space Station (ISS), the Carbon Dioxide Removal Assembly (CDRA) has been the primary system for CO_2 control [2]-[6]. CDRA is a 4-bed molecular sieve system that operates with two sets of beds that alternately sorb and desorb CO_2 using thermal/pressure swing cycles. Cabin air is sent through the first of one 2-bed series, where water vapor is removed by desiccant material (Sylobead and 13X zeolite). Once dried and conditioned, the air is sent through the second bed where most CO_2 is removed by adsorbent zeolite 5A pellets. The treated air is then re-humidified by passing it through the desorbing desiccant bed to recover the trapped water. Heating the removal bed drives the CO_2 from the zeolite for compression and delivery to downstream processes (e.g. a Sabatier reactor for recovery of oxygen). Exposing the CO_2 removal adsorbent to the vacuum of space desorbs any remaining gases.

Historically, CDRA has been able to maintain the partial pressure of CO_2 ($ppCO_2$) in the cabin atmosphere from about 2 to 5 mm Hg (267 to 667 Pa) with 7-day averages of 3.4 mm Hg [7]. Long-term continuous exposure to elevated CO_2 concentrations has been hypothesized to adversely affect crew performance and contribute to crew physiological issues (headaches, vision impairment, and intracranial pressure) [1], [7]-[11]. Astronaut performance and comfort can begin to degrade as early as 2.3 to 2.7 mm Hg $ppCO_2$ [1]. Allen et al. determined that 1,400 ppm CO2 (1.1 mm Hg ppCO2) in ventilated indoor spaces adversely affected cognition [12]. In response to these concerns, astronauts and physicians have advocated for lower levels. The ISS has reduced the maximum allowable level to 4 mm Hg $ppCO_2$. Further reduction to levels below 2 mm Hg $ppCO_2$ are desired to keep the risk of headache below 1% [7]. For these reasons, physicochemical technologies with potential to meet this goal have been under investigation.

Several regenerable sorbent materials have been researched for CO_2 removal from space habitat atmospheres, which include zeolite-coated Microlith mesh substrates [13], zeolite sorbent materials [3]-[6], [13]-[15], liquid and solid amines [16]-[17], and ionic liquids [18]. Implementations for treatment of spacecraft cabin or spacesuit atmospheres include the CO_2 Removal and Compression System (CRCS) [19], the CO_2 And Moisture Removal Amine Swing-bed (CAMRAS) [16], the Rapid Cycling Amine (RCA) system [17], Supported Ionic Liquid Membranes (SILMs) [20]-[23], and water walls, a novel passive concept in which a supported water wall absorbs gases from the

cabin atmosphere for provision to algae [24]. Each of these sorbents are described below.

A. Zeolite Sorbents

Zeolites, often called molecular sieves because they can separate gas molecules by size, are microporous sorbents used for gas separation and purification processes [25]. Composition of the zeolite can thermodynamically or kinetically favor selective separation of gases [26]. The zeolite sorbent can be regenerated by applying heat (temperature swing), reducing the pressure (pressure swing) or both to drive off the adsorbed gas.

CDRA uses a packed bed of CaA (5A) zeolite pellets with 5Å pore size for CO_2 removal from spacecraft cabin atmospheres [3]-[6], [14]-[15]. However, since the 5A zeolite favors sorption of water vapor over CO_2, the cabin air first passes through a NaX zeolite (13X, 10Å pore size) pellet bed to control humidity. The 5A zeolite also has another drawback; the CO_2 loading decreases with lower partial pressure. At 25°C and 267 Pa ppCO_2, the 5A zeolite saturates at 3.4 g CO_2/100 g sorbent. The loading drops to less than 2 g CO_2/100 g at 133 Pa [27]. Recent work [28], [29] screened alternative zeolite sorbents for mechanical integrity and recovery of CO_2 capacity after exposure to moisture. Grade 544 13X zeolite had faster adsorption kinetics with improved capacity than 5A zeolites.

B. Solid Amine Sorbents

The Shuttle Regenerative Carbon Dioxide Removal System (RCRS) used solid amine-coated ion resin beads. A polymeric resin (e.g. acrylic, polystyrene or divinylbenzene) was coated with a CO_2 adsorbing amine such as monoethanolamine (MEA), diethanolamine (DEA), or methyldiethanolamine (MDEA). Filburn et al. [30] later found SA9T amine-coated porous plastic ion-exchange beads to have increased capacity over the RCRS solid amine sorbent, although exposing the amines to space vacuum may result in a loss of sorbent to thereby reduce CO_2 removal capability over time [16]. This same SA9T sorbent has since been used in the CO_2 And Moisture Removal Amine Swing-bed (CAMRAS) [16] and the Rapid Cycling Amine (RCA) systems, which have packed beds and flow paths similar to other pellet-based CO_2 removal beds [17]. CAMRAS was selected for use in Orion. The RCA system is being considered for the next generation spacesuit CO_2 removal and humidity control system.

C. Monoethanolamine

Terrestrially, MEA has been considered for scrubbing CO_2 from exhaust gases [31]-[32] and onboard submarines [33]. In the former application, a CO_2-laden gas is sparged through the MEA solvent to preferentially remove CO_2 gas. Regeneration of the MEA occurs by stripping the CO_2 via a sweep gas at elevated temperature (100-200°C if using steam) [34]. However, there is generally concern for using liquid (supported or unsupported) amines in a spacecraft cabin due to corrosion, amine degradation and the possibility of forming and releasing toxic ammonia gas during desorption [34]. CO_2 sorption with MEA approaches equilibrium (0.5 moles CO_2/mole MEA or 36 g CO_2/100 g MEA) consistent with a global expression (Eq (1)) for the reaction mechanism [35].

$$CO_2 + 2RNH_2 \rightleftharpoons RNH_3^+ + RNHCO_2^- \quad (1)$$

D. Room Temperature Ionic Liquids (RTILs)

Room temperature ionic liquids (RTILs) are complex salts that by definition are liquid at room temperature and remain in liquid form over a wide range of temperatures and pressures [18]. They have negligible vapor pressure, are generally stable from 0 to 200°C and thus, are not expected to degrade or produce toxic vapors at conditions necessary for regenerable CO_2 sorption [36]. Several ILs have been identified and developed that have high solubility for CO_2 (on the same order as amine solvents at ~30 w% and higher) over a range of partial pressures. Together, the anion and cation molecules comprising the IL determine its physical properties, such as viscosity and diffusivity, which in turn affects its capacity for CO_2 uptake and mass transport.

Imidazolium-based ILs have shown high selectivity for CO_2 sorption over nitrogen and oxygen (depending on the nature of the anion and/or functional groups), allowing them to selectively uptake CO_2 without drastically changing the remaining gas composition whether for revitalization of spacecraft atmospheres [20]-[23], [36]-[41], control of greenhouse gas emissions [42]-[48], or natural gas treatment [49]-[50]. The RTIL, 1-butyl-3-methylimidazolium acetate [bmim][Ac] (Fig. 1), readily and reversibly uptakes CO_2 through both physical and chemical sorption [51]-[52]. Mixtures with CO_2 uptake of nearly 20 w% exhibits almost no vapor pressure suggesting the formation of a chemical complex with the ionic liquid [53]. Chemical formation of 1-butyl-3-methylimidazolium-2-carboxylate was identified in a room temperature mixture of CO_2 and pure non-aqueous [bmim][Ac] [54]. Kortunov et al [55] confirm the chemical pathway via ^{1}H NMR. Although, for approximately 70 w% 1-ethyl-3-imidazolium acetate in deionized water, the authors report the absence of C-carboxylation.

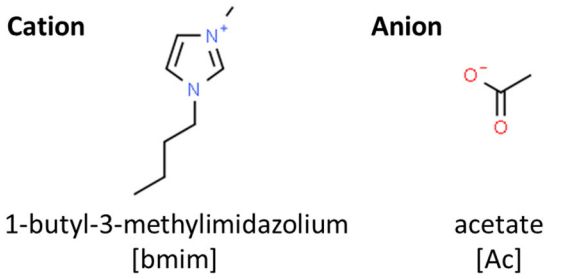

Fig. 1. 1-butyl-3-methylimidazolium acetate ([bmim][Ac]).**

CO_2 uptake may increase viscosity, and thereby the power required to pump the IL. It could also negatively affect the rate of CO_2 uptake by slowing the diffusion kinetics and convective transport. [Bmim][Ac] was chosen for its relatively low magnitude of CO_2-saturated increased viscosity. No more than 10 mPa-s difference with CO_2-saturated [bmim][ac] was observed with respect to the CO_2-free value of 406 mPa-s (all measurements made at 23°C ± 1°C), indicating that saturation with CO_2 should not negatively affect the ability to pump or flow the IL through membrane contactors. The capacity of [bmim][Ac] for CO_2 sorption along with relevant thermophysical properties reported here (Table 1).

Table 1. Physical properties of [bmim][Ac] at 25°C unless otherwise specified.

	This Work 23±1°C	Literature 25±0.1°C	Reference
Density (kg/m^3)	Not measured	1052.59	[56]
Viscosity (mPa-s)	406 ± 4	428 ± 0.5[a]	[57], [58]
Specific heat (J/kg-K)	Not measured	1922.23	[56]
Electrical conductivity (mS/cm)	0.639	0.5221	[59]
CO_2 diffusivity (m^2/s)		1.99 x 10^{-11}	[60]
w% CO_2 at 84.1 kPa	7.45 ± 0.1	7.62 ± 0.07[b]	[52], [61]

[a] linear interpolation of viscosity assuming 2 w% water
[b] linear interpolation of CO_2 sorption at 84.1 kPa

Because [bmim][Ac] absorbs CO_2 using both chemical and physical means, its uptake capacity exceeds that expected from Henry's law [51]. A CO_2-laden atmosphere (0.27 kPa ppCO_2 in an ideal gas mixture at those same conditions) comprises 0.26 mol% of CO_2, yet from an extrapolation of solubility data [52]-[61], the ionic liquid [bmim][Ac] is expected to absorb as much as 5.6 mol% (1.3 w%) before reaching saturation. At conditions of 101.3 kPa and 25°C, the maximum uptake of CO_2 in [bmim][Ac] will be 27.5 mol% (7.77 w%). Even a 23 w% aqueous solution with [bmim][Ac] absorbed 6.88 w% (25.0 mol%) CO_2 after 60 minutes of sparge at 84 kPa and 295.1 K [62]. The uptake of CO_2 by the aqueous solution at partial pressures of 63, 42, 21 and 0 kPa CO_2 with balance of argon are also reported.

RTILs can continually remove CO_2 from spacecraft and spacesuit atmospheres when used in a supported ionic liquid membrane [20]-[23] or direct liquid contactor [36]-[41] given subsequent removal from the permeate flow to maintain a difference in partial pressures, the driving potential for gas transport. Membrane supports can be either organic (polymeric) or inorganic (ceramic or metallic), porous or non-porous. The pores of polymeric flat sheet and hollow fiber membranes are infiltrated with an RTIL to produce a supported liquid membrane (SLM). The CO_2-laden

** Molecular structures from chemspider.com, http://www.chemspider.com/Chemical-Structure.13095209.html?rid=2204aa9b-8097-437e-91f5-9a701f456b77 <accessed 3 Jan 2020>.

air can flow through either the lumen or shell side of the contactor. By using a sweep gas or vacuum on the opposing side, these membranes continuously separate CO_2 from the atmosphere with high selectivity. Permeance, the rate of volumetric flux of the solute gas across the membrane for a given pressure gradient, is a defining metric for SLM performance. Both the membrane structure and liquid sorbent affect permeance. The membrane through pore size and tortuosity. Greater capacity for gas sorption and faster diffusivity through the liquid will increase permeance. Importantly, some ILs have been shown to facilitate CO_2 permeance under conditions of reduced $ppCO_2$ in the feed stream [20].

One direct liquid contactor, Carbon Dioxide Removal by Ionic Liquid Sorbent (CDRILS) flows an ionic liquid (both [emim][Ac] and [bmim][Ac] have been studied) through the lumen side of a hollow fiber contactor to remove CO_2 from the gas flow passing over the fibers on the shell side [36]-[39]. Arquilla et al. [40] describe designs for a flat plate contactor, a 3-D printed capillary-driven contactor and a hollow fiber contactor that use the ionic liquid [bmim][Ac] for CO_2 removal. Unlike the CDRILS contactor, this group's hollow fiber membrane contactor passed the CO_2 laden gas stream through the lumen side of the fibers and the RTIL was pumped through the shell side. In another concept, 3-D printed pipes were designed with interior capillary flow tubes for support and circulation of liquids to an air-liquid interface in microgravity. Using ILs as the CO_2 capture solvent, these pipes could enable passive CO_2 capture and humidity control at ambient temperatures and pressures [41].

In this paper, we present the results of experiments to characterize CO_2 removal from simulated spacecraft cabin atmospheres using the gas-liquid membrane contactors of Arquilla et al. [40]. We also report experiments to characterize CO_2 desorption from the ionic liquid [bmim][Ac].

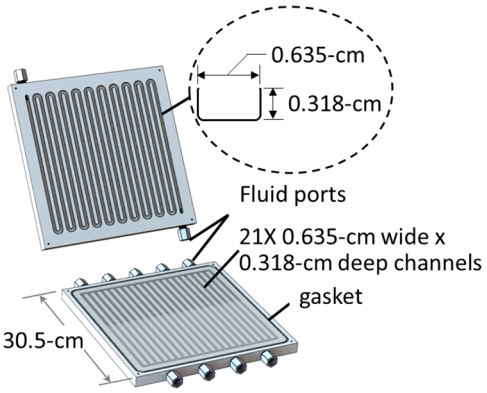

a) Flat plate contactor

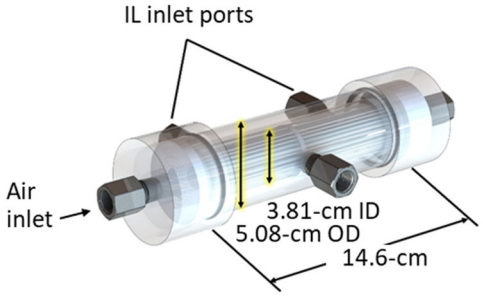

b) Hollow fiber contactor

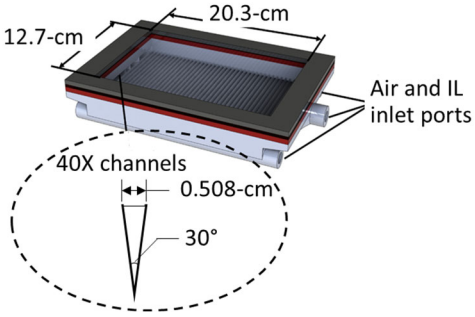

c) Interior corner capillary contactor

Fig. 2. Gas-liquid contactors after Arquilla et al. [40] for CO_2 removal from simulated space habitat cabin atmospheres.

II. Experimental

A. CO_2 Removal with IL-based Contactors

Three gas-liquid membrane contactors (Fig. 2) were constructed for the characterization of CO_2 removal using [bmim][Ac]. A flat plate membrane contactor was used as a control, due to its simple geometry. A hollow fiber contactor has large surface area-to-volume ratio and can work in both microgravity and gravity environments. As long as the Concus-Finn condition is met for the advancing contact angle, an interior corner capillary contactor can function in a microgravity environment despite having a free surface [63].

Candidate materials for construction were exposed to the ionic liquid for several weeks, which was deemed sufficient to assess suitability for the two-week test entry. Viscosities (falling ball viscometer, Gilmont EW-08702-10) and electrical conductivities (Omega CDH-280 conductivity meter) were measured to inform the effects of material interactions on the composition of [bmim][ac] samples, while visual observations of the IL color were also noted.

1. Test Articles

The custom built flat plate membrane contactor (Fig. 2a) has twenty-one 0.635-cm-wide x 0.318-cm-deep x 26.1-cm long parallel channels for the liquid flow and a single 0.635-cm-wide x 0.318-cm-deep serpentine channel for the gas

flow. The article provides 348 cm^2 surface area. The surface area-to-volume ratio of this contactor is 160 m^2 m^{-3}. The serpentine flow path was chosen to increase gas residence time and increase the CO_2 transport across the 0.0127-cm-thick hydrophobic silicone membrane (SSPM823-008, Interstate Specialty Products). The contactor housing was machined in-house from ultra-high molecular weight polyethylene (UHMWPE).

The custom hollow fiber contactor (Fig. 2b) had 118 porous polypropylene fibers, each with an outer diameter of 0.065-cm, an inner diameter of 0.039-cm, and a wall thickness of 0.014-cm. The wetted length of the fibers was 14.6-cm. In total, the fibers provide 352 cm^2 surface area. This contactor has a surface area-to-volume ratio of 210 m^2 m^{-3}, whereas densely-packed hollow fiber configurations have ratios that typically range from 500 to 9,000 m^2 m^{-3} [64]. The CO_2 gas permeable fibers have a porosity of 60-70% (manufacturer supplied information, pore size not known). The hydrophobic polypropylene does not allow [bmim][Ac] to infiltrate the fiber pores. Fibers were supported between two polypropylene guides and UHMWPE end caps. A third polypropylene guide maintained separation between the suspended fibers. Polyurethane adhesive (H.B. Fuller®, UR-2187 A/B) and Buna-N o-rings sealed the gas and liquid flow paths. Silicone tubing (L/S 15 Masterflex) flowed [bmim][Ac] to and from the shell-side of the contactor. The assembly fit within an UHMWPE housing.

The interior corner capillary contactor (Fig. 2c) has forty 0.508-cm-wide x 12.7-cm-long channels with 30° included angle (15° half angle). The interior corner channels readily wet and advance the [bmim][Ac] through the contactor bed. Surface tension allows the ionic liquid to creep up the sides of each channel and form a liquid surface (approximately 258 cm^2 surface area) for direct contact with the CO_2-laden atmosphere flowing across the bed. The surface area-to-volume ratio of this contactor is 80 m^2 m^{-3}. The contactor was additive manufactured using a proprietary polycarbonate-type resin (VisiJet SL Clear, 3D Systems, Rock Hill, South Carolina). A silicone gasket sealed a polycarbonate window between the contactor and an acrylic lid.

Key characteristics of each membrane contactor are given in Table 2. The contact surface area applies to the interface between the CO_2-laden gas and ionic liquid. The potential for use in gravity and microgravity environment are also indicated for each. Only the hollow fiber and interior corner contactors are designed for use in microgravity (uG) environments.

Table 2. Characteristics of the gas-liquid contactors.

	Geometric Features	**Principal Materials of Construction**	**Contact Surface Area (cm^2)**	**Potential Use Environment**
Flat plate	21X 0.635-cm-wide x 0.33-cm deep liquid channels 1X 0.635-cm-wide x 0.33-cm deep serpentine channel for gas flow	Ultra high molecular weight polyethylene (UHMWPE)	348	Gravity environments
Hollow fiber	118 hollow fibers 0.065 cm OD x 0.039 cm ID	Polypropylene and UHMWPE	352	uG and gravity environments
Interior corner capillary	40X 0.508-cm-wide liquid channels with 15° half angle	Polycarbonate	258	uG environment

2. Method and Apparatus

Each contactor was characterized using the Atmospheric and Environmental Test Hub for Experimentation on Revitalization (AETHER) test rig in the CU Boulder Bioastronautics Laboratory. AETHER can simulate and deliver space habitat cabin atmospheres to a test article. Fig. 3 shows the process diagram for contactor testing. Nominally, a metered, dry gaseous N_2 stream with 2.0 mm Hg $ppCO_2$ (3,200 ppm CO_2 at 84 kPa local atmospheric pressure) was provided to each membrane contactor for characterization of CO_2 removal. Although the capability exists, the feed stream of CO_2-laden gas was not humidified. An Omega FMA-1607A-V2P flow meter measured the gas flow rates which were parametrically varied from 0.2 to 0.7 slpm (reference conditions of 25°C and 14.7 psia). Inlet and outlet concentrations of CO_2 were measured using non-dispersive infrared (NDIR) CO_2 sensors (GC-0012, CozIR®). Inlet gas pressure and temperature were measured with Honeywell 140PC15 S112 and Vaisala HMP 110 sensors, respectively.

Fresh, stock [bmim][Ac] (assay 97.4% pure with 1.73% water, Sigma-Aldrich CAS 284049-75-8, lot number BCBM4905V) was loaded into each contactor for the set of CO_2 removal experiments. CO_2 was not desorbed from

the IL as the accumulative uptake over the course of the experiment was estimated to be negligible in comparison to the initial loading of 1.67 w% level. A peristaltic pump (Masterflex model 07554-90 L/S Economy Drive with 77200-62 L/S Easy-Load II Pump Head, Cole-Parmer Item # EW-77910-20) controlled the flow of [bmim][Ac] through the contactors. This flow was varied from 50 to 400 mL/min. A 16-bit LabVIEW data acquisition and control system (National Instruments™ M Series Multifunction DAQ) acquired and stored data at approximately 0.8 Hz.

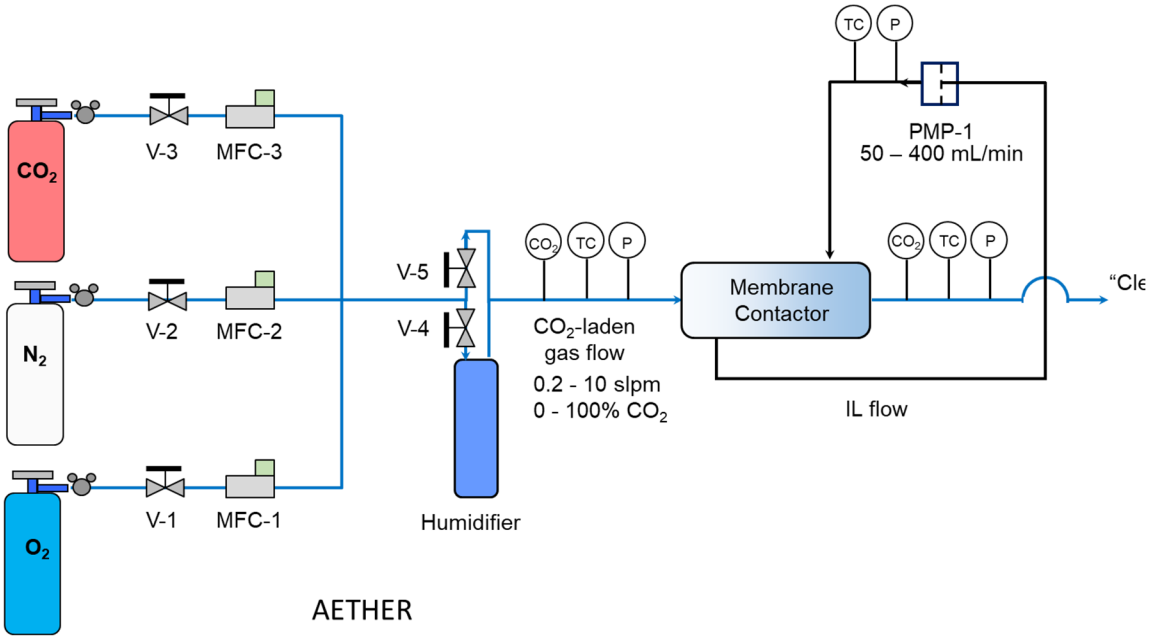

Fig. 3. Process and instrumentation diagram for testing of membrane contactors.

3. Calculations

The molar flux $\dot{N}$ is proportional to the concentration difference ($c_i|_{gas} - c_i|_{IL}$). This proportionality, denoted by k, is the overall mass transfer coefficient [65].

$$\dot{N} = k \cdot \frac{(c_i|_{gas} - c_i|_{IL})}{1E06} \cdot \frac{p}{R_u \cdot T}|_{gas} \qquad (mol\ m^{-2}\ s^{-1}) \tag{2}$$

k	overall mass transfer coefficient (m s-1)
$c_i\|_{gas}$	average concentration of species i at the interface (ppm)
$c_i\|_{IL}$	concentration in bulk solution (ppm), assumed negligible
p	static pressure of the gas (84,100 Pa)
R_u	universal gas constant (8.315 J mol^{-1} K^{-1})
T	gas temperature (297 K)

Then, the mass flux G is obtained by multiplying the molar flux $\dot{N}$ by the molecular weight of CO_2 ($\mathcal{M}_{CO2}$ = 44.01 g mol^{-1}).

$$G = \dot{N} \cdot \mathcal{M}_{CO2} \cdot 86{,}400\ s/day \qquad (g\ m^{-2}\ day^{-1}) \tag{3}$$

B. CO_2 Desorption from [bmim][Ac]

1. Preparation of CO_2-laden [bmim][Ac]

Glassware, except the Pyrex® tray and 500 mL beaker, were cleaned and washed using a three step process between every experimental run. Washes progressed from tap water, to filtered deionized water, and then isopropyl alcohol. Beakers and flasks were wiped dry with Kimwipes® between each wash, while fritted glass bubblers (Prism Research Glass) were left to air dry.

Water and dissolved gasses were removed from the stock [bmim][Ac] at elevated temperature under vacuum for up to 47 hours. A 125 mL Pyrex flask containing the IL was immersed in a water bath held at a temperature between 70 and 80°C on a hot plate (Bante Instruments MS300) with closed loop control. A two-stage vacuum pump (CPS Products Inc Pro Set VP2D) was connected to the sidearm of the flask through a liquid trap with wire reinforced plastic tubing. The pressure in the side arm flask was held between approximately 40 and 75 Pa. Time, temperature (digital temperature gauge, Omega HH42A), pressure (digital vacuum gauge, Omega OVG64), and mass (analytical balance, Cole-Parmer Symmetry PA-224) were recorded at 1/2 to 2 hour intervals. From these measurements, the RTIL mass, the change of mass each measurement interval, accumulative loss of mass, and rate of mass loss were determined. The rate of mass loss was used as an indicator for the progression of water removal from the ionic liquid. About two hours after initiation of the thermal vacuum drying process, the loss rate reached an approximately constant value of 0.03 w% per hour. At 6 hours, and after removal of 1 w% water from the solution, the drying process was stopped and the IL stored under rough vacuum (≤ 2.7 Pa) until use.

Fig. 4 presents the apparatus for saturation of ionic liquid with CO_2. CO_2 gas (Airgas, 99.999%) was sparged through a fritted glass bubbler into the 'dried' ionic liquid at 95 mL/min (Alicat mass flow controller). The sparge gas agitated the IL eliminating the need for a stir plate. Pressure and temperature within the beaker were ambient (84.1 kPa, 23°C). Excess CO_2 exhausted to the atmosphere. At 30 to 60 minute intervals, the bubbler was disconnected from the gas flow and the combined mass of the beaker, bubbler, and IL was obtained. The sparge process was continued until the CO_2 uptake exceed 7.30 w%. At laboratory temperature (23 ± 1°C), [bmim][Ac] should uptake 7.62 ± 0.07 w% CO_2 before reaching saturation (estimated from [52]). Neat [bmim][Ac] was added to a known mass of dry, CO_2-saturated [bmim][Ac] in order to lower the CO_2 concentration to 1.67 w%, equivalent to saturation in a 630 mm Hg (84.1 kPa) atmosphere with 2 mm Hg partial pressure CO_2. The resulting solution was then used to study methods for desorption of CO2 from the IL.

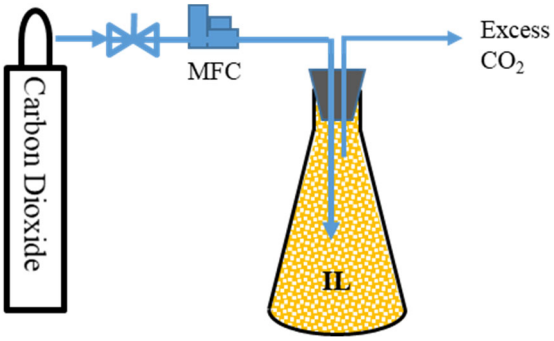

Fig. 4. Apparatus for sparging CO_2 into ILs.

Viscosities of stock and CO_2-laden [bmim][Ac] were measured with a falling ball viscometer (Gilmont EW-08702-10). Viscosities of the latter were no more than 10 mPa-s greater than 406 mPa-s for the stock IL at 23°C.

2. Methods and Apparatus for CO_2 Desorption

Two methods for CO_2 desorption are described: thermal vacuum and thermal sparge desorption.

a. Thermal Vacuum Desorption

A side arm flask with known mass of [bmim][Ac] loaded with 1.67 w% CO_2 was connected via vacuum hose to the CPS ProSet VP2D two-stage vacuum pump (Fig. 5). A stopper sealed the top of the flask. A second flask served as a liquid trap. An Omega DVG-64 vacuum gauge measured rough vacuum pressure (circa 500 microns Hg). All connections between the components were coated with vacuum grease. Hose clamps secured and sealed the vacuum hose to connections on the vacuum pump and vacuum gauge. The flask was placed in a water bath on a hot plate (Bante Instruments MS300) set to the desired temperature. An integrated thermal probe controlled the bath temperature. Neither the ionic liquid or water bath were agitated or stirred. Sous vide (PVC) 20-mm-dia balls were used to cover the water in order to limit evaporation. Pressure, temperature and total mass were recorded at regular intervals. During the first hour of desorption, the IL was observed to bubble vigorously which was thought to be remaining volatile impurities as well as CO_2 coming out of solution.

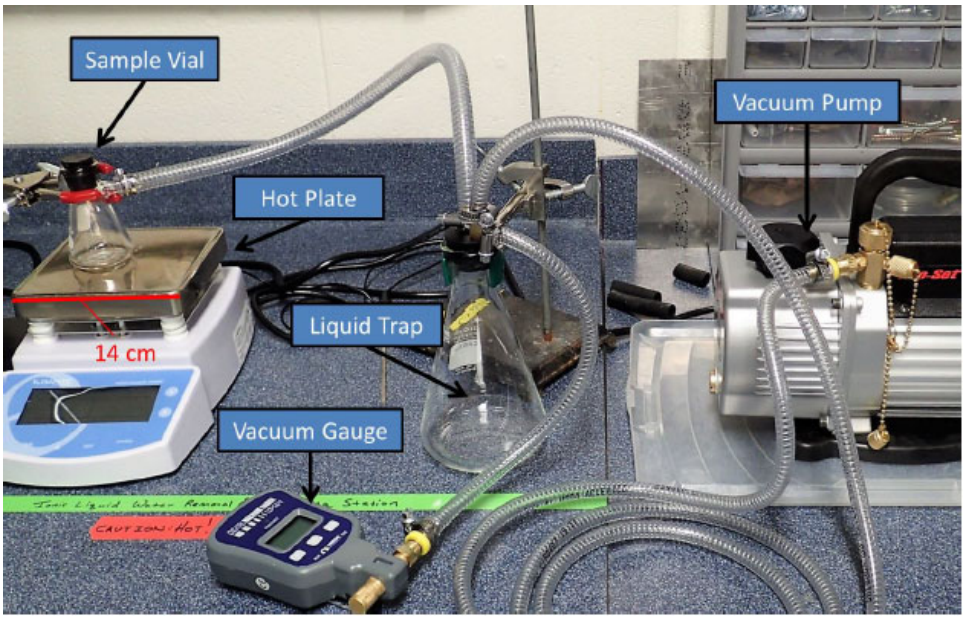

Fig. 5. CO_2 desorption setup. Water bath not included for clarity.

b. Desorption via Inert Gas Sparge

CO_2 sparge desorption setup used an argon gas (Airgas, >99.5% pure) handling system connected to a side arm flask that was vented to the atmosphere, nominally 84.1 kPa and 23°C (Fig. 6). A mass flow controller (Alicat Scientific MCE-100SCCM-D/5M) metered a 95 mL/min flow of argon through the bubbler and into the ionic liquid. The IL was not stirred by any other means. At 30 to 60 minute intervals, the argon flow rate and water bath temperature were recorded. For gravimetric measurements, the bubbler was disconnected from the argon flow, the flask removed from the hot water bath and wiped dry, and then its mass recorded on the analytical balance before being returned to the water bath and the argon reconnected to resume sparge desorption.

Fig. 6. Assembly for sparge desorption of CO_2 from [bmim][Ac].

C. Quantification of Uncertainty

The uncertainty of a measured parameter δx was estimated from the root-sum square of both the precision δS_i and bias δB_j errors using Eq (4), where the indices i and j represent unique sources of error.

$$\delta x = \frac{t}{\sqrt{N}}\sqrt{\sum_i \left(\delta S_i\right)^2} + \sqrt{\sum_j \left(\delta B_j\right)^2} \quad (4)$$

with t the value assuming a two-sided Student-t distribution with $\alpha = 0.025$ and $\nu = N\text{-}1$ to attain 95% confidence of the uncertainty on the measurements. Measurement uncertainties were then propagated through Eq (5) to obtain the uncertainty U_Z of a derived performance parameter Z. The derivative of Z with respect to the measured parameter x captures the influence (or significance) of that parameter's uncertainty with respect to the parameter Z. The uncertainty U_Z then results from the root-sum square of contributions from the measured parameters x.

$$U_Z = \sqrt{\sum_x \left(\frac{\partial Z}{\partial x}\,\delta x\right)^2} \quad (5)$$

The Cole-Parmer Symmetry PA-224 specifies that a measurement is repeatable to 0.2 mg ($\frac{t}{\sqrt{N}}\sqrt{\sum_i (\delta S_i)^2}$ = 0.2 mg) and the overall linearity for the balance is also 0.2 mg (δB_1 = 0.2 mg). Thus, a single measurement has an uncertainty of 0.4 mg. The uncertainty on change of mass Δm due to gas sorption and/or desorption is ±0.57 mg given an influence coefficient $\frac{\partial \Delta m}{\partial m}$ of 1.0. Sufficient quantities of [bmim][Ac], about 50 g, were used to keep the uncertainties on CO_2 sorption and desorption below ±0.010 w%.

The Omega FMA-1607A-V2P flow meters have an accuracy of 0.8% of reading plus 0.2% full-scale. The CozIR GC-0012 CO_2 sensors are accurate to ± 50 ppm or ±3% of reading, whichever is greater. Linearity is < 1% of full scale (10,000 ppm) or ±100 ppm, which can contribute to both precision and bias errors. Sensitivity to pressure is 0.13% of reading per 133 Pa in normal atmospheric conditions (approximately ±0.26% bias error at 267 Pa ppCO_2 or 3,200 ppm CO_2 at 0.0841 MPa, the Boulder local atmosphere). The National Instruments M series data acquisition module records data with 12-bit accuracy, which introduces negligible error (±0.24% full scale on measurements). By averaging at least 30 samples, the influence of precision errors is significantly reduced, and the uncertainty on CO_2 concentration measurements within the gas stream is expected to be less than ± 203 ppm at 3,200 ppm CO_2 and less than ± 138 ppm at 1,000 ppm CO_2.

III. Results and Discussion

A. Material Compatibility

The compatibility of stock [bmim][Ac] with eight polymeric materials was assessed (Fig. 7).

- Ultra-high molecular weight polyethylene (UHMW PE),
- polytetrafluoroethylene (PTFE),
- polypropylene (PP),
- nylon,
- fluorinated ethylene propylene (FEP),
- polyvinylidene fluoride (PVDF),
- Tygon®, and
- Versilon™

Fig. 7. Material compatibility samples compared to a control; 23°C ± 1°C.

After several weeks, only PVDF and Tygon materials exhibited a visual color change with respect to the control due to interaction with [bmim][Ac]. Viscosity and electrical conductivity measurements were made at 23°C ± 1°C to quantitatively assess the stock samples of [bmim][Ac] after material exposure (Table 3). The control sample had a viscosity of 406 mPa-s. Based upon the manufacturer specification for repeatability, the error was estimated between ±0.2 and ±1.0% (approx. 4 mPa-s). As seen in Table 4, the viscosities of [bmim][Ac] were lower after exposure to the materials. Electrical conductivity, a measure of ion mobility, was 0.639 ± 0.006 mS/cm for the control. Values outside this range suggest an interaction between the material and the [bmim][Ac] even though no visual change was observed. Material interactions with [bmim][Ac] and water could have released organic solvents such as toluene, ethanenitrile, dichloomethane and benzene that affect viscosity [18] and electrical conductivity.

Table 3. Material compatibility test results.

	Control	UHMW PE	PTFE	PP	Nylon	FEP	PVDF	Tygon	Versilon
Color	Light yellow	Light yellow	Light yellow	Light yellow	Light yellow	Light yellow	Brown	Dark brown	Light yellow
Viscosity (mPa-s)	406	301	387	348	352	358	367	349	379
Electrical conductivity (mS/cm)	0.639	---	0.612	0.656	0.625	0.625	0.617	0.391	0.637

B. CO_2 Removal from Simulated Spacecraft Cabin Atmospheres

Contactor performance is characterized by the measured concentration differences (Fig. 8) and calculations of the mass flux (Fig. 9). At the end of each set of experiments, the total uptake of CO2 by [bmim][Ac] was calculated and found to be less than 5% of its 1.67 w% capacity for CO2 sorption at the test conditions. At most this would impart a 5% degradation in mass transport over the course of the experiment. Our estimates for uncertainty on CO_2 concentrations, rates of removal and mass transport coefficients accounted for this factor.

The rank order of the contactors based on these attributes is:

Interior corner capillary > hollow fiber > flat plate

The interior corner capillary and hollow fiber membrane contactors had similar capabilities for reduction of the CO_2 concentration level within the simulated cabin atmospheres. At 0.24 slpm gas flow, CO_2 levels were lowered from the inlet condition of 3,200 ppm ± 800 ppm to less than 1,000 ppm at the outlet. However, the interior corner capillary contactor achieved this reduction with greater transport of CO_2 (approximately 60 g m^{-2} day^{-1} as compared to 40 g m^{-2} day^{-1} for the hollow fiber contactor and 18 g m^{-2} day^{-1} for the flat plate contactor). The results also show the influence of cabin atmosphere and IL flows on CO_2 removal. For all contactors, slower gas flow rates (i.e. longer residence times) achieve a greater difference in concentration (Fig. 8a) and thus, a greater reduction of the CO_2 concentration level in the simulated cabin atmosphere at the contactor exit, even though the mass flux rate of CO_2 removal remained nearly constant for the range of gas flows tested (Fig. 9a). Except for the interior corner capillary contactor, varying the IL flow rate from 50 to 400 mL/min had little effect on CO_2 transport. Both the concentration differences (Fig. 8b) and removal rates (Fig. 9b) were relatively insensitive to the flow of IL through the contactor.

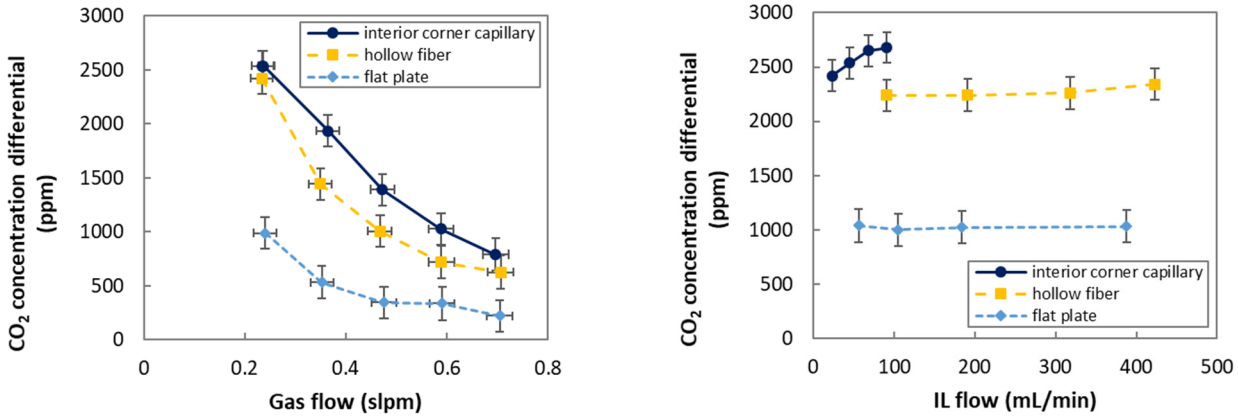

a) effect of gas flow (45, 91, 110 mL/min IL flows for interior corner, hollow fiber and flat plate contactors, respectively)

b) effect of IL flow (0.24 slpm gas flow)

Fig. 8. Absolute difference in CO_2 concentrations from the inlet (nominally 3,200 ppm in the simulated cabin atmosphere) to the outlet of the membrane contactors.

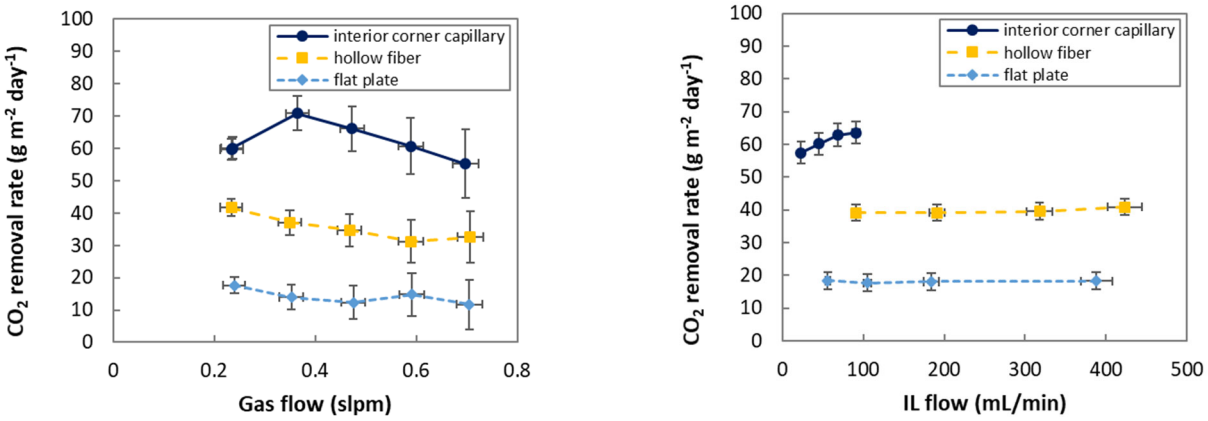

a) effect of gas flow (45, 91, 110 mL/min IL flows for interior corner, hollow fiber and flat plate contactors, respectively)

b) effect of IL flow (0.24 slpm gas flow)

Fig. 9. Flux rates of CO_2 removal by the contactors.

Using Eqs (4) and (5) we calculated the overall mass transfer coefficients *k* (Fig. 10). The mass transfer coefficients for each contactor decrease with increased gas flow (Fig. 10a), yet with the exception of the hollow fiber contactor were insensitive to increased IL flow rate (Fig. 10b). It was expected that the laminar flow Reynolds number and therefore also the Sherwood number and mass transfer coefficient would increase with a greater flow of IL. The largely insensitivity of *k* to the IL flow rate suggests that another mechanism (e.g. gas diffusion through the porous membrane or the laminar boundary layer) has limited CO_2 transport.

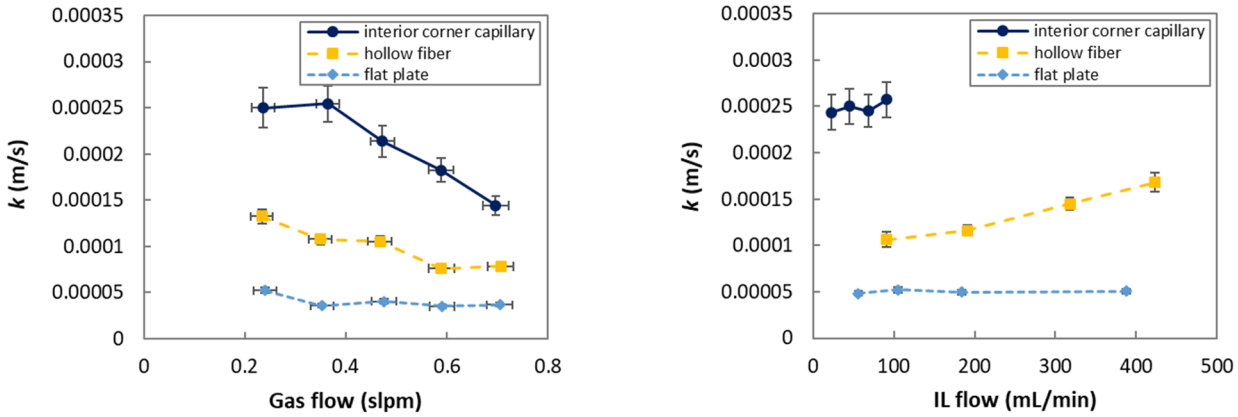

a) effect of gas flow (45, 91, 110 mL/min IL flows for interior corner, hollow fiber and flat plate contactors, respectively)

b) effect of IL flow (0.24 slpm gas flow)

Fig. 10. Experimentally determined overall mass transfer coefficients k for the membrane contactors.

At 0.24 slpm feed flow and the optimum IL flow rate tested, the overall mass transfer coefficients *k* were (5.2 ± 0.3) x 10^{-5} m s-1, (16.8 ± 1.3) x 10^{-5} m s-1 and (25.0 ± 1.9) x 10^{-5} m s-1 for the flat plate, hollow fiber and interior corner contactors, respectively. The value for the interior corner contactor was at its design flow for capillarity of 45 mL/min. In general, the coefficients were observed to decrease in direct proportion to increased gas flow. This performance metric was nearly insensitive to variations in the flow of ionic liquid.

Table 4 compares these experimental results to those derived from analytical models [40] for test conditions of 0.24 slpm gas flow and IL flows less than 100 mL/min. The analytical models significantly underpredicted mass transport for all contactor configurations. In addition, our mass transfer coefficient for the hollow fiber membrane

contactor falls between those from Yates et al. [37] for CO_2 removal with commercial (Microza Membranes) and proprietary membranes. The mass transfer coefficient for the latter (7.80×10^{-4} m s^{-1}) suggests that the membrane material, porous structure and geometry are important to mass transfer since the liquid, gas and CO_2 concentrations were held constant.

Table 4. Comparison of mass transfer coefficients (m s-1) for [bmim][Ac] contactors.

	This work[a]	Arquilla et al. [40][a,b]	Yates et al. [37][c]	Santos et al. [60][d]
Flat Plate	$(5.2 \pm 0.3) \times 10^{-5}$	2.8×10^{-5}	---	5.65×10^{-6}
Hollow Fiber	$(16.8 \pm 1.3) \times 10^{-5}$	3.6×10^{-5}	2.17×10^{-5} (commercial) 7.80×10^{-4} (proprietary)	
Interior Corner Capillary	$(25.0 \pm 1.9) \times 10^{-5}$	6.7×10^{-5}	---	

[a] 0.24 slpm gas flow.
[b] Calculated from the analytical predictions for CO_2 difference between inlet and outlet concentrations in the gas flow.
[c] 90:10 molar ratio of [bmim][Ac]:water as the sorbent, and with carrier gas of air at atmospheric pressure laden with 1 to 4 mm Hg partial pressure of CO_2.
[d] SILM contactor with pure CO2 feed gas at 0.45 bar pressure differential and 298K

The mass transfer results are also compared to the literature (Table 5). Coefficients are reported for CO_2 removal from challenge atmospheres using ionic-liquid based hollow fiber membrane contactors. The values span more than two orders of magnitude (from 1.0×10^{-6} m/s to 7.80×10^{-4} m/s) dependent upon the liquid sorbent, CO_2-laden atmosphere fed to the membrane contactor, operating conditions and membrane contactor features (not reported here). The highest mass transfer was obtained with [bmim][Ac] in solution with water which at 10 vol% lowers the viscosity while nearly retaining the same capacity for CO_2 sorption as the neat IL at room temperature [66]. Elevating the temperature also increases mass transfer through increased chemisorption phenomenon, lower viscosity and higher diffusivity [47].

Table 5. Comparison with literature values for hollow fiber membrane contactors with other ILs.

Sorbent	Feed Gas Stream (Vol %)	P (atm)	T (°C)	k (m s^{-1})	Reference
[bmim][Ac]	0.32/99.68 CO_2/N_2	0.83	23±1	$(16.8 \pm 1.3) \times 10^{-5}$	This work
[bmim][Ac]:H_2O [a]	0.13 to 0.72 CO_2/balance air	1.0	[f]	78×10^{-5}	[37]
[bmim][TCM] [b]	45/55 CO_2/He	19.74	80	0.1×10^{-5}	[43]
[dmpdah][Ac]:H_2O [c]	10/90 CO_2/air	1.0	20	$(3.71 \pm 0.2) \times 10^{-5}$	[45]
[emim][$EtSO_4$] [d]	15/85 CO_2/N_2	1.02	18	3.99×10^{-5}	[46]
[emim][$EtSO_4$]	15/85 CO_2/N_2	[f]	25	0.071×10^{-5}	[48]
[emim][Ac] [e]	15/85 CO_2/N_2	[f]	30	1.66×10^{-5}	[47]
[emim][Ac]	15/85 CO_2/N_2	[f]	25	0.11×10^{-5}	[48]

[a] 1-butyl-3-methylimidazolium acetate + 10% H_2O
[b] 1-butyl-3-methlyimidazolium tricyanomethanide
[c] dimethylpropylenediamine acetate + 50% H_2O
[d] 1-ethyl-3-methylimidazolium ethylsulfate
[e] 1-ethyl-3-methylimidazolium acetate
[f] not reported, presumed laboratory conditions

Each contactor considered here can be scaled for application to space habitats, although ones with low mass and volume will be desired. Using the highest empirically determined values for the rate of CO_2 removal by each contactor, Table 6 summarizes the surface area and volume needed to remove 1.037 kg CO_2/day. Estimates for the mass assumed a density of 420 kg m^{-3} calculated from CDRA data [38].

Table 6. Contactor sizing.

	CO_2 removal rate ($g\ m^{-2}\ day^{-1}$)	Surface Area (m^2)	Surface Area to Volume Ratio ($m^2\ m^{-3}$)	Volume (m^3)	Mass (kg)
Flat Plate	18	58	160 [40]	0.36	150
Hollow Fiber	42	25	3000, based on [64]	0.0082	3.5
Interior Corner Capillary	71	15	80 [40]	0.18	77

The hollow fiber contactor will have the highest surface area to volume ratio (a value was assumed for this analysis that was midway within the 500 to 9000 $m^2\ m^{-3}$ reported by Seader and Henley [64]). The volume of a single contactor should only be about 0.0082 m^3 to remove the CO^2 respired by one crewmember in one day. In comparison, the packaging of flat membrane and free liquid surfaces will be much less efficient requiring substantially greater volumes on the order of 0.18 to 0.36 m^3. Their relatively large volume and mass will likely make them unattractive for crewed spacecraft, although the simplicity of the interior corner capillary contactor warrants its consideration in design trade studies. As points of comparison, CDRA and the CDRILS membrane contactors have the capability to support a crew of four and yet have volumes of 0.44 m^3 and 0.093 m^3, respectively [38]. An assembly comprising two hollow fiber membrane contactors based upon this work (0.016 m^3) should compare favorably to CDRILS when infrastructure and support equipment are included.

C. CO_2 Desorption

Desorption experiments via thermal vacuum were conducted at temperatures ranging from ambient to 80°C. The desorption results on w% basis are plotted in Fig. 11. 155 mg of mass were lost over 4.5 hours at 22°C (a rate of 34 mg CO_2/h). Although some water may have been driven from the solution, this loss of mass was attributed to desorption of CO_2 from the solution. At 71°C, the average loss rate had increased to 67 mg CO_2/h. At 81°C, the average rate of loss had increased further to 105 mg CO_2/h. These results are thought to be diffusion-rate limited as the vacuum desorption apparatus did not have provision for stirring.

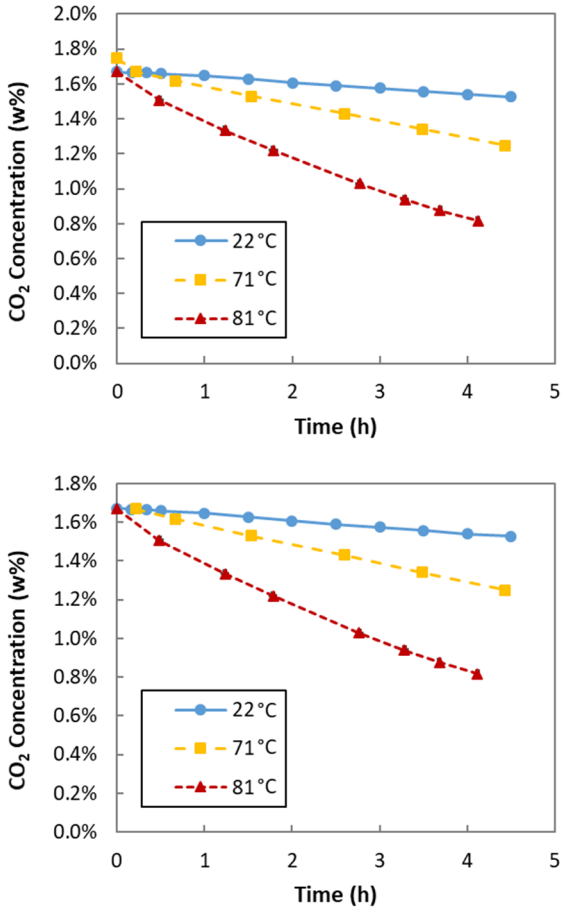

Fig. 11. CO_2 desorption via thermal vacuum.

Gas sparge desorption experiments were conducted at room and elevated temperatures (Fig. 12). At room temperature (19°C), an initial increase of 10.8 mg was observed during the first hour due to sorption of Ar gas. From that point forward, a net decrease in system mass of 74 mg over the next 2.7 hours was measured which is attributed to loss of CO_2 from the solution. The average loss rate was 27 mg CO_2/h. At 65°C, the average rate of loss increased to 94-102 mg CO_2/h. It is expected that further increase in temperature or higher sparge gas flow rate would increase the rate of desorption.

Analysis of results from the two methods suggests that sparge desorption outperformed vacuum desorption. After 4 hrs at 71°C and rough vacuum (68 Pa), gravimetric measurements indicated a decrease in loading of CO_2 from 1.75 w% to 1.29 w%. In comparison, for a 95 ml/min gas sparge flow through CO_2 saturated [bmim][Ac] at the cooler temperature of 65°C, the loading decreased from 1.67 w% to 0.75 w% over the same period of time. It should be noted that stirring the CO_2-laden IL would likely have increased the rate of desorption under vacuum.

Other considerations include the influence of operating conditions and method on power demand and stability of the ionic liquid. [Bmim][Ac] needs 1922 J kg^{-1} K^{-1} to raise its temperature. The lower the desorption temperature, the less power needed for heating and greater likelihood for holding the IL below its threshold for thermal stability (approx. 120°C for [bmim][Ac] [60]). In addition, both desorption methods require power in proportion to the volumetric flow of gases and the pressure differential. Vacuum desorption has a much lower flow of gas to work on as primarily drawing CO_2 from solution, but has a one atmosphere pressure differential. The sparge method moves a higher flow of gas with only a small increase in pressure to overcome the viscous resistance of the IL. Further development will be needed to determine which method will need less power.

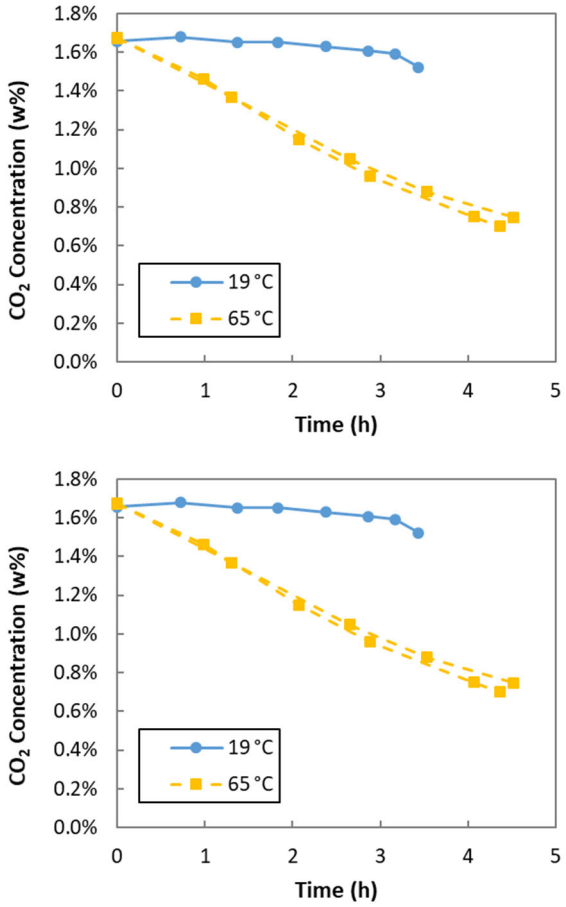

Fig. 12. CO_2 sparge desorption.

IV. Conclusions

The capacity of an IL-based CO_2 removal system for revitalization of spacecraft cabin atmospheres depends upon several factors: the rate of mass transfer from gas to liquid and rate of desorption from the liquid. The first is directly proportional to the difference between its saturated capacity at the desired atmospheric concentration and the amount of CO_2 remaining in solution after regeneration. Three contactors were experimentally characterized for efficacy of [bmim][Ac] to remove CO_2 from a simulated space habitat atmosphere with 2 mm Hg ppCO_2. All three reduced the level of CO_2 with the interior corner capillary being most effective ($k = 25.0 \times 10^{-5}$ m s^{-1}, 60 g CO_2 m^{-2} day^{-1}), the hollow fiber next ($k = 16.8 \times 10^{-5}$ m s^{-1}, 41 g CO_2 m^{-2} day^{-1}) and a flat plate configuration the least effective ($k = 5.2 \times 10^{-5}$ m s^{-1}, 18 g CO_2 m^{-2} day^{-1}). The interior corner capillary contactor has advantages over the other two configurations: 1) it does not need a physical membrane to separate the ionic liquid from the gas stream which is expected to facilitate a greater rate of sorption and 2) ideally, capillarity will wet the contactor surface with the IL. The contactor only needs power to pump liquid to or from the contactor surface. However, the interior corner capillary contactor will not package as well as a hollow fiber membrane contactor. Its ratio of surface area-to-volume was 80 m^2/m^3 whereas densely packed hollow fiber configurations have ratios that are from one to two orders of magnitude greater. A preferred configuration for a given application will likely depend upon the trade between these metrics and thus, both the interior corner capillary and hollow fiber contactors warrant scale up for further study.

The reversible uptake of CO_2 with an IL depends upon its efficacy for desorption, which in turn will ultimately determine the feasibility for use in a regenerable CO_2 removal system. CO_2 does not readily desorb at ambient temperature, so thermal vacuum and inert gas sparge methods were evaluated for desorption of CO_2 from the ionic

liquid [bmim][Ac] as appear feasible for integration within space habitat architectures. Further both methods should be feasible to use with the contactors investigated here, although data are not yet available to determine if the surface area employed for CO2 removal will later be sufficient for desorption. Of the two, inert gas sparge provided twice the desorption rate of thermal vacuum for similar operating temperatures (circa 70°C). Thus, an inert gas sparge offers potential for faster regeneration and greater reversible uptake at elevated temperature than thermal vacuum. Future work should investigate feasibility for use of these desorption methods with hollow fiber and interior corner capillary contactors.

Funding Sources

This research was supported in part by the National Space Grant Foundation under the auspice of NASA's Exploration Habitation (X-Hab) 2017 Academic Innovation Challenge. Award XHab 2017-04.

Acknowledgments

The authors thank Dr. Mark Weislogel's research group at Portland State University for design of the interior corner capillary channels.

References

[1] Anderson, M. S., Ewert, M. K., and Keener, J. F., "Life Support Baseline Values and Assumptions Document," NASA/TP-2015–218570/REV1, Jan 2018. https://ntrs.nasa.gov/archive/nasa/casi.ntrs.nasa.gov/20180001338.pdf.

[2] Cmarik, G. E., and Knox, J. C., "CO2 Removal for the International Space Station – 4-Bed Molecular Sieve Material Selection and System Design," ICES-2019-5, 49th International Conference on Environmental Systems, Jul 2019. https://hdl.handle.net/2346/84429.

[3] Knox, J. C., and Stanley, C. M., "Optimization of the Carbon Dioxide Removal Assembly (CDRA) in Support of the International Space System and Advanced Exploration Systems," ICES-2015-165, 45th International Conference on Environmental Systems, Jul 2015. http://hdl.handle.net/2346/64432.

[4] Reysa, R. P., Lumpkin, J. P., El Sherif, D., Kay, R., and Williams, D. E., "International Space Station (ISS) Carbon Dioxide Removal Assembly (CDRA) Desiccant/Adsorbent Bed (DAB) Orbital Replacement Unit (ORU) Redesign," SAE Technical Paper 2007-01-3181, Jul 2007. https://doi.org/10.4271/2007-01-3181.

[5] El Sherif, D., and Knox, J. C., "International Space Station Carbon Dioxide Removal Assembly (ISS CDRA) Concepts and Advancements," SAE Technical Paper 2005-01-2892, Jul 2005. https://doi.org/10.4271/2005-01-2892.

[6] Knox, J. C., "International Space Station Carbon Dioxide Removal Assembly Testing," SAE Technical Paper 001CES-234, Jan 2000. https://doi.org/10.4271/2000-01-2345.

[7] Law, J., Van Baalen, M., Foy, M., Mason, S. S., Mendez, C., Wear, M. L., Meyers, V. E., and Alexander, D., "Relationship Between Carbon Dioxide Levels and Reported Headaches on the International Space Station," Journal of Occupational and Environmental Medicine, **56** (5) May 2014, pp. 477-483. https://doi.org/10.1097/JOM.0000000000000158.

[8] James, J. T., Meyers, V. E., Sipes, W., Scully, R. R., and Matty, C. M., "Crew Health and Performance Improvements with Reduced Carbon Dioxide Levels and the Resource Impact to Accomplish Those Reductions," AIAA-2011-5047, 41st International Conference on Environmental Systems, Jul 2011. https://doi.org/10.2514/6.2011-5047.

[9] Scully, R. R., Basner, M., Nasrini, J., Lam, C., Hermosillo, E., Gur, R. C., Moore, T., Alexander, D. J., Satish, U., and Ryder, V. E., "Effects of acute exposures to carbon dioxide on decision making and cognition in astronaut-like subjects," npj Microgravity **5**, 17 (2019). https://doi:10.1038/s41526-019-0071-6.

[10] Matty, C. M., "Overview of Carbon Dioxide Control Issues During International Space Station/Space Shuttle Joint Docked Operations," AIAA 2010-6251, 40th International Conference on Environmental Systems, Jul 2010. https://doi.org/10.2514/6.2010-6251.

[11] Law, J., Watkins, S., and Alexander, D., "In-Flight Carbon Dioxide Exposures and Related Symptoms: Association, Susceptibility, and Operational Implications," NASA/TP–2010–216126, Jun 2010.

[12] Allen, J. G., MacNaughton, P., Satish, U., Santanam, S., Vallarino, J. and Spengler, J. D., "Associations of Cognitive Function Scores with Carbon Dioxide, Ventilation, and Volatile Organic Compound Exposures in Office Workers: A Controlled Exposure Study of Green and Conventional Office Environments," Environmental Health Perspectives, 124 (6), Jun 2016, pp. 805-812. https://doi.org/10.1289/ehp.1510037.

[13] Junaedi, C., Roychoudhury, S., Howard, D., Perry, J., and Knox, J., "Microlith-based Structured Sorbent for Carbon Dioxide, Humidity, and Trace Contaminant Control in Manned Space Habitats," AIAA-2011-5215, 41st International Conference on Environmental Systems, Jul 2011. https://doi.org/10.2514/6.2011-5215.

[14] Watson, D., Knox, J. C., West, P., Stanley, C. M., and Bush, R., "Sorbent Structural Impacts Due to Humidity on Carbon Dioxide Removal Sorbents for Advanced Exploration Systems," ICES-2015-166, 45th International Conference on Environmental Systems, Jul 2015. http://hdl.handle.net/2346/64433.

[15] Knox, J. C., Gauto, H., and Miller, L. A., "Development of a Test for Evaluation of the Hydrothermal Stability of Sorbents used in Closed-Loop CO_2 Removal Systems," ICES-2015-200, 45th International Conference on Environmental Systems, Jul 20. http://hdl.handle.net/2346/6447215.

[16] Button, A., and Sweterlitsch, J., "Amine Swingbed Payload Testing on ISS," ICES-2014-063, 44th International Conference on Environmental Systems, Jul 2014. http://hdl.handle.net/2346/59626.

[17] Chullen, C., Campbell, C., Papale, W., Hawes, K., and Wichowski, R., "Rapid Cycle Amine 3.0 System Development," ICES-2015-313, 45th International Conference on Environmental Systems, Jul 2015. http://hdl.handle.net/2346/64543.

[18] Seddon, K. R., Stark, A., and Torres, M.-J., "Influence of chloride, water, and organic solvents on the physical properties of ionic liquids," Pure and Applied Chemistry, **72** (12), 2000, pp. 2275–2287. https://doi.org/10.1351/pac200072122275.

[19] Richardson, T.-M. J., Jan, D., Hogan, J., Palmer, G., Koss, B., Samson, J., Huang, R., and Knox, J., "Progress on the CO2 Removal and Compression System," ICES-2015-064, 45th International Conference on Environmental Systems, Jul 2015. http://hdl.handle.net/2346/64460.

[20] Hanioka, S., Maruyama, T., Sotani, T., Teramoto, M., Matsuyama, H., Nakashima, K., Hanaki, M., Kubota, F., and Goto, M., "CO2 separation facilitated by task-specific ionic liquids using a supported liquid membrane," Journal of Membrane Science, **314** (1-2), Apr 2008, pp. 1–4. https://doi.org/10.1016/j.memsci.2008.01.029.

[21] Wickham, D., Nabity, J., McCarty, J., and Aaron, R., "A Supported Liquid Membrane System for Steady State CO_2 Control in a Spacecraft Cabin," ICES-2019-187, 49th International Conference on Environmental Systems, July 2019. https://hdl.handle.net/2346/84954.

[22] Wickham, D. T., Gleason, K. J., Engel, J. R., and Cowley, S. W., "Continued Advancement of Supported Liquid Membranes for Carbon Dioxide Control in Extravehicular Activity Applications," ICES-2015-164, 45th International Conference on Environmental Systems, Jul 2015. http://hdl.handle.net/2346/64431.

[23] Wickham, D. T., Gleason, K. J., Engel, J. R., Cowley, S. W., and Chullen, C., "Advanced Supported Liquid Membranes for Carbon Dioxide Control in Extravehicular Activity Applications," ICES-2014-231, 44th International Conference on Environmental Systems, Jul 2014. http://hdl.handle.net/2346/59694.

[24] Cohen, M. M., Matossian, R. L., Mancinelli, R. L., Flynn, M. T., "Water Walls Life Support Architecture," AIAA-2013-3517, 43rd International Conference on Environmental Systems, Jul 2013. https://doi.org/10.2514/6.2013-3517.

[25] Handbook of Zeolite Science and Technology, 1st edition, Scott M. Auerbach, Kathleen A. Carrado, Prabir K. Dutta editors, CRC Press, Published July 31, 2003, pp. 1063-1104. https://doi.org/10.1201/9780203911167.

[26] Singh, V. K., and Kumar, E. A., "Comparative Studies on CO_2 Adsorption Kinetics by Solid Adsorbents," Energy Procedia **90** (2016) p. 316 – 325. https://doi.org/10.1016/j.egypro.2016.11.199

[27] Mulloth, L. M., and Finn, J. E., "Carbon Dioxide Adsorption on a 5A Zeolite Designed for CO_2 Removal in Spacecraft Cabins," NASA/TM-1998-208752, 1998. http://link.library.in.gov/resource/dC-5oj5-lRo/.

[28] Knox, J. C., Watson, D. W., Giesy, T. J., Cmarik, G. E., and Miller, L. A., "Investigation of Desiccants and CO_2 Sorbents for Exploration Systems 2016-2017," ICES-2017-188, 47th International Conference on Environmental Systems, Jul 2017. http://hdl.handle.net/2346/72993.

[29] Mattox, E. M., Knox, J. C., Bardot, D.M., "Carbon dioxide removal system for closed loop atmosphere revitalization, candidate sorbents screening and test results," Acta Astronautica, **86**, May–June 2013, pp. 39-46. https://doi.org/10.1016/j.actaastro.2012.09.019.

[30] Filburn, T., Nalette, T., and Graf, J., "The Design and Testing of a Fully Redundant Regenerative CO2 Removal System (RCRS) for the Shuttle Orbiter," SAE Technical Paper 2001-01-2420, 2001. https://doi.org/10.4271/2001-01-2420.

[31] Botheju, D., Hovland, J., Haugen, H. A., and Bakke, R., "Monoethanolamine biodegradation processes," Proceedings of the 2nd Annual Gas Processing Symposium, p. 77-86. https://doi.org/10.1016/S1876-0147(10)02009-4.

[32] Wang, L., Zhang, Z., Zhao, B., Zhang, H., Lu, X. and Yang, Q., "Effect of long-term operation on the performance of polypropylene and polyvinylidene fluoride membrane contactors for CO2 absorption," Separation and Purification Technology, vol. 116, 2013, pp. 300-306. https://doi.org/10.1016/j.seppur.2013.05.051.

[33] Emergency and Continuous Exposure Guidance Levels for Selected Submarine Contaminants: Volume 1. The National Academies Press, ISBN-13: 978-0-309-09225-8, 2007. https://doi.org/10.17226/11170.

[34] Olajire, A. A., "CO2 capture and separation technologies for end-of-pipe applications – A review," Energy, **35** (6) 2010, p. 2610-2628. https://doi.org/10.1016/j.energy.2010.02.030.

[35] Xie, H.-B., Zhou, Y., Zhang, Y., Johnson, J. K., "Reaction Mechanism of Monoethanolamine with CO_2 in Aqueous Solution from Molecular Modeling," The Journal of Physical Chemistry A 2010, 114 (43) pp. 11844-11852. https://doi.org/10.1021/jp107516k.

[36] Yates, S. F., Bershitsky, A., Bonk, T., Henson, P., and MacKnight, A., "Direct Liquid Contact -- Next Generation Approach to Combined CO2 Recovery and Humidity Control for Extended Missions," AIAA SPACE 2016, American Institute of Aeronautics and Astronautics, AIAA-2016-5462, 2016. https://doi.org/10.2514/6.2016-5462.

[37] Yates, S. F., Bershitsky, A., Kamire, R. J., Henson, P., Bonk, T., and Isobe, J., "A Closed-Loop CO2 and Humidity Recovery System for Deep Space Missions," ICES-2017-20, 47th International Conference on Environmental Systems, Jul 2017. http://hdl.handle.net/2346/72867.

[38] Yates, S. F., Kamire, R. J., Henson, P., and Bonk, T., "Carbon Dioxide Removal by Ionic Liquid Sorbent (CDRILS) System Development," ICES-2018-17, 48th International Conference on Environmental Systems, Jul 2018. http://hdl.handle.net/2346/74035.

[39] Yates, S. F., Kamire, R. J., Henson, P., Bonk, T., Loeffelholz, D., Zaki, R., Fox, E., Kaukler, W. and Henry, C., "Scale-up of the Carbon Dioxide Removal by Ionic Liquid Sorbent (CDRILS) System," ICES-2019-219, 49th International Conference on Environmental Systems, Jul 2019. https://hdl.handle.net/2346/84442.

[40] Arquilla, K., Rundle, T., Shaffer, B., Phillips, D., Lampe, A., Denton, J., Fritz, T., Lima, A., Dixon, J., Lotto, M., Holquist, J., and Nabity, J., "Characterization of Carbon Dioxide Removal using Ionic Liquids in Novel Geometries," ICES-2017-234, 47th International Conference on Environmental Systems, July 2017. http://hdl.handle.net/2346/73030.

[41] Graf, J., Weislogel, M., and Brennecke, J., "Thirsty Walls - A new paradigm for air revitalization in life support," NASA Final Technical Report, NNH-15ZOA001N-15NIAC, https://www.nasa.gov/sites/default/files/atoms/files/niac_graf_thirstywalls_phase1_2015_final_report.pdf <accessed 3 Jan 2020>

[42] Dai, Z., Noble, R. D., Gin, D. L., Zhang, X., and Deng, L., "Combination of ionic liquids with membrane technology: A new approach for CO2 separation," Journal of Membrane Science, vol. 497, Jan. 2016, pp. 1–20. https://doi.org/10.1016/j.memsci.2015.08.060.

[43] Dai, Z. and Deng, L., "Membrane absorption using ionic liquid for pre-combustion CO2 capture at elevated pressure and temperature," International Journal of Greenhouse Gas Control, vol. 54, part 1, November 2016, pp. 59-69. https://doi.org/10.1016/j.ijggc.2016.09.001.

[44] Lu, S.-C., Khan, A.L. and Vankelecom, I.F.J., "Polysulfone-ionic liquid based membranes for CO2/N2 separation with tunable porous surface features," Journal of Membrane Science, vol. 518, 2016, pp. 10-20. https://doi.org/10.1016/j.memsci.2016.06.031.

[45] Simons, T.J., Hield, P. and Pas, S.J., "A novel experimental apparatus for the study of low temperature regeneration CO2 capture solvents using hollow fibre membrane contactors," International Journal of Greenhouse Gas Control, vol. 78, 2018, pp. 228-235. https://doi.org/10.1016/j.ijggc.2018.08.009.

[46] Qazi, S., Gómez-Coma, L., Albo, J., Druon-Bocquet, S., Irabien, A. and Sanchez-Marcano, J., "CO2 capture in a hollow fiber membrane contactor coupled with ionic liquid: Influence of membrane wetting and process parameters," Separation and Purification Technology, vol. 233, 2020. https://doi.org/10.1016/j.seppur.2019.115986.

[47] Gómez-Coma, L., Garea, A., Rouch, J.C., Savart, T., Lahitte, J.F., Remigy, J.C. and Irabien, A., "Membrane modules for CO2 capture based on PVDF hollow fibers with ionic liquids immobilized," Journal of Membrane Science, vol. 498, 2016, pp. 218-226. https://doi.org/10.1016/j.memsci.2015.10.023.

[48] Gómez-Coma, L., Garea, A. and Irabien, A., "Non-dispersive absorption of CO2 in [emim][EtSO4] and [emim][Ac]: Temperature influence," Separation and Purification Technology, vol. 132, 2014, pp. 120-125. https://doi.org/10.1016/j.seppur.2014.05.012.

[49] Wickramanayake, S., Hopkinson, D., Myers, C., Hong, L., Feng, J., Seol, Y., Plasynski, D., Zeh, M. and Luebke, D., "Mechanically robust hollow fiber supported ionic liquid membranes for CO2 separation applications," Journal of Membrane Science, vol. 470, 2014, pp. 52-59. https://doi.org/10.1016/j.memsci.2014.07.015.

[50] Mohshim, D.F., Mukhtar, H. and Man, Z., "A study on carbon dioxide removal by blending the ionic liquid in membrane synthesis," Separation and Purification Technology, vol. 196, 2018, pp. 20-26. https://doi.org/10.1016/j.seppur.2017.06.034.

[51] Domínguez, C. M., Munoz, M., Quintanilla, A., Pedro, D., M, Z., Ventura, S. P. M., Coutinho, J. A. P., Casas, J. A., and Rodriguez, J. J., "Degradation of imidazolium-based ionic liquids in aqueous solution by Fenton oxidation," Journal of Chemical Technology and Biotechnology, **89** (8), Aug 2014, pp. 1197–1202. https://doi.org/10.1002/jctb.4366.

[52] Yokozeki, A., Shiflett, M. B., Junk, C. P., Grieco, L. M., and Foo, T., "Physical and Chemical Absorptions of Carbon Dioxide in Room-Temperature Ionic Liquids," The Journal of Physical Chemistry B, vol. 112, Dec. 2008, pp. 16654–16663. https://doi.org/10.1021/jp805784u.

[53] Shiflett, M. B., Kasprzak D. J., Junk, C. P. and Yokozeki, A., "Phase behavior of {carbon dioxide + [bmim][Ac]} mixtures," J. Chem. Thermodynamics, 40 (2008) pp. 25–31. https://doi.org/10.1016/j.jct.2007.06.003

[54] Besnard, M., Cabaco, M. I., Chavez, F. V., Pinaud, N., Sebastiao, P. J., Coutinho, J. A. P., and Danten, Y., "On the spontaneous carboxylation of 1-butyl-3-methylimidazolium acetate by carbon dioxide," Chemical Communications, **48** (9), 2012, pp. 1245–1247. https://doi.org/10.1039/c1cc16702b.

[55] Kortunov, P. V., Saunders Baugh, L. and Siskin, M. "Pathways of the Chemical Reaction of Carbon Dioxide with Ionic Liquids and Amines in Ionic Liquid Solution," Energy Fuels **29** (9), Jul 2015, pp. 5990-6007. https://doi.org/10.1021/acs.energyfuels.5b00876

[56] Safarov, J., Geppert-Rybczyn´ska, M., Kul, I., and Hassel, E., "Thermophysical properties of 1-butyl-3-methylimidazolium acetate over a wide range of temperatures and pressures," Fluid Phase Equilibria, 383 (2014) pp. 144–155. https://doi.org/10.1016/j.fluid.2014.10.015.

[57] Fendt, S., Padmanabhan, S., Blanch, H. W., and Prausnitz, J. M., "Viscosities of Acetate or Chloride-Based Ionic Liquids and Some of Their Mixtures with Water or Other Common Solvents," Journal of Chemical Engineering Data, 2011, **56** (1), pp. 31–34. https://doi.org/10.1021/je1007235.

[58] Fredlake, C. P., Crosthwaite, J. M., Hert, D. G., Aki, S. N. V. K., Brennecke, J. F. "Thermophysical properties of imidazolium-based ionic liquids," Journal of Chemical Engineering Data, 2004, **49** (4), pp. 954–964. https://doi.org/10.1021/je034261a.

[59] Kanakubo, M., Makino, T. and Umecky, T., "CO2 solubility in and physical properties for ionic liquid mixtures of 1-butyl-3-methylimidazolium acetate and 1-butyl-3-methylimidazolium bis(trifluoromethanesulfonyl)amide," Journal of Molecular Liquids, 217 (2016) pp. 112-119. https://doi.org/10.1016/J.MOLLIQ.2016.02.018.

[60] Santos, E., Albo, J. and Irabien, A., "Acetate based Supported Ionic Liquid Membranes (SILMs) for CO2 separation: Influence of the temperature," Journal of Membrane Science, Volume 452, 15 February 2014, pp. 277-283. https://doi.org/10.1016/j.memsci.2013.10.024.

[61] Shiflett, M. B., Kasprzak, D.J., Junk, C.P., and Yokozeki, A., "Phase Behavior of {Carbon Dioxide + [BMIM][Ac]} Mixtures," Journal of Chemical Thermodynamics, **40** (1), 2008, pp. 25-31. https://doi.org/10.1016/j.jct.2007.06.003.

[62] Lotto, M.A., Nabity, J.A. and Klaus, D.M. (20XX), Low Pressure CO2 Capture using Ionic Liquids to Enable Mars Propellant Production, Journal of Propulsion and Power [Revised Manuscript Submitted].

[63] Weislogel, M. M., and Lichter, S., "Capillary flow in an interior corner," Journal of Fluid Mechanics, 373, 1998, pp. 349–378. https://doi.org/10.1017/S0022112098002535

[64] Seader, J.D. and Henley, E.J., Separation Process Principles, John Wiley and Son, Inc. New York, 1998.

[65] Sirkar K.K. (1992) Other New Membrane Processes. In: Ho W.S.W., Sirkar K.K. (eds) Membrane Handbook. Springer, Boston, MA. https://doi.org/10.1007/978-1-4615-3548-5_46.

[66] Stevanovic, S., Podgoršek, A., Pádua, A. A. H. and Gomes, M. F. C., "Effect of Water on the Carbon Dioxide Absorption by 1-Alkyl-3-methylimidazolium Acetate Ionic Liquids," J. Phys. Chem. B 2012, **116** (49) pp. 14416-14425. https://doi.org/10.1021/jp3100377.